N94- 34980

Departure Solutions of the Unsteady Thin-Layer and Full Navier-Stokes Equations Solved Using Streamline Curvature Based Iteration Techniques

M. Barnett
United Technologies Research Center
East Hartford, Connecticut

D. Turner and A. P. Rothmayer
Iowa State University
Ames, Iowa

Abstract

The development of a thorough understanding of the mechanisms for vortex eruptions from viscous layers, which are believed to be associated with phenomena such as dynamic stall onset and transition, is crucial if accurate models of such phenomena are to be formulated. The development of such models may, in turn, allow for the possibility that such effects could be accounted for during the design of various aerodynamic devices such as wings, helicopter rotors and turbomachinery blading and thus lead to designs which are stall free or stall resistant and which have better stall-recovery properties. The present investigation is being conducted as part of an effort to develop analytical and numerical tools which can be used to help improve our understanding of the vortex-eruption mechanism at high Reynolds numbers. The addition of the normal-momentum equation to the classical unsteady boundary-layer equations is crucial, according to recent asymptotic analyses of the vortex-eruption problem, and is a key feature of the analyses being developed by the present authors. The purpose of this paper is, first, to describe departure solution behavior observed when using unsteady, streamline-curvature based solution procedures in which nontrivial transverse pressure gradient effects are included and, second, to show that special treatment of the time-derivative of the normal velocity is needed to eliminate the ill-posed solution behavior, which is observed when small spatial and temporal step sizes are used.

Introduction

A number of recent analytical studies have been directed towards understanding the fundamental physics associated with the development and subsequent eruption of concentrated regions of vorticity from the boundary layer (e.g., van Dommelen and Shen (1980), Elliott, *et al* (1983), Peridier, *et al* (1988) and Smith (1988)). This event is believed to be associated with well-known physical phenomena, such as the onset of airfoil dynamic stall and transition from laminar to turbulent flow. The cumulative observation of the above-mentioned and other studies seems to indicate that the classical boundary-layer equations are insufficient to completely describe the vortex eruption phenomenon. Even if strong viscous-inviscid interaction is allowed, it appears likely that normal pressure gradient effects must be accounted for in some form. The present paper describes part of an overall effort directed towards the development of unsteady analyses capable of addressing high Reynolds number flows in which normal pressure gradients are important and ultimately, it is hoped, where vortex eruptions occur, as well.

The important work of van Dommelen and Shen (1980) first documented the existence of a finite-time singularity in the solution of the non-interacting, classical, unsteady boundary-layer equations for flow past an impulsively started circular cylinder. Later work (e.g., Peridier, *et al* (1988)) showed that, if the boundary-layer equations are allowed to interact with the inviscid flow, the van Dommelen and Shen singularity can be bypassed. However, another finite-time singularity, which cannot be removed through interaction alone, arises shortly thereafter. The recent asymptotic study of Smith (1988) indicates that normal pressure gradient effects must be included in order to avoid the latter (interactive) finite-time singularity. This provides the motivation for the present work, which addresses the issue of how various terms in the unsteady normal-momentum equation must be numerically treated within the framework of a globally iterated space- and time-marching solution algorithm, in order to avoid ill-posed behavior of the solutions. Globally iterated solution algorithms for steady and unsteady flows have been employed extensively in both asymptotic (*i.e.*, infinite Reynolds number) and finite Reynolds number investigations, where they have proven to be computationally

efficient. Streamline curvature techniques have been demonstrated in a number of studies, for example, see Smith *et al* (1984), Presz (1985), Rothmayer (1989, 1990) and Power (1990) – many other examples can be found in the literature. Thus, this approach is being pursued here in the hope that the use of a boundary-layer like numerical approach will lead to a computationally efficient technique to solve the vortex-eruption problem.

External Flow Analysis – Flow Past a Flat Plate

The particular concern of this paper is an issue which arose while the first author was developing a numerical solution scheme for the equation set consisting of the classical, unsteady, incompressible boundary-layer equations supplemented with the inviscid form of the normal-momentum equation. Note that these equations are essentially identical to the leading-order terms in the Incompressible form of the "Thin-Layer" Navier-Stokes equations, and will therefore be referred to here as the ITLNS equations, for convenience. For two-dimensional flows these equations are given by

$$\frac{\partial u}{\partial x} + \frac{\partial v}{\partial y} = 0 \ , \tag{1}$$

$$\frac{\partial u}{\partial t} + u\frac{\partial u}{\partial x} + v\frac{\partial u}{\partial y} = -\frac{\partial P}{\partial x} + \frac{\partial^2 u}{\partial y^2} \tag{2}$$

and

$$\frac{\partial v}{\partial t} + u\frac{\partial v}{\partial x} + v\frac{\partial v}{\partial y} = -Re\frac{\partial P}{\partial y} \ , \tag{3}$$

where u and v are the velocity components in the x- and y-directions, respectively, with x oriented tangent to the body surface and y normal to it, and P is the static pressure. In this section, the body is assumed to be a semi-infinite flat plate, so that x and y are Cartesian coordinates. Standard low-speed, external flow nondimensionalizations have been used and the y-coordinate and v-velocity component have been scaled with the square root of the Reynolds number as follows: $u = u^*/U^*_\infty$, $v = v^*\sqrt{Re}/U^*_\infty$, $P = (P^* - P^*_\infty)/\rho^* U^{*2}_\infty$, $x = x^*/L^*_{ref}$, $y = y^*\sqrt{Re}/L^*_{ref}$ and $t = t^*/(L^*_{ref}/U^*_\infty)$. Asterisks denote dimensional quantities, the subscript ∞ denotes a quantity evaluated in the uniform far field upstream flow and Re is the Reynolds number defined as $Re = U^*_\infty L^*_{ref}/\nu^*$, where ν^* is the upstream value of the kinematic viscosity which, along with the density ρ^*, is assumed to be constant.

The ITLNS equations can be solved in the primitive variable form given above, or they can be solved after transforming to Görtler variables – the latter approach has been used in this study. However, to simplify the present discussion, the primitive variable form of these equations will be considered, after using the stream function ψ, defined by the relations $u = \partial\psi/\partial y$ and $v = -\partial\psi/\partial x$, to replace v. Substituting for v in Eq. (3) yields

$$-\frac{\partial^2\psi}{\partial x\partial t} - u\frac{\partial^2\psi}{\partial x^2} + \frac{\partial\psi}{\partial x}\frac{\partial^2\psi}{\partial x\partial y} = -Re\frac{\partial P}{\partial y} \ . \tag{4}$$

The boundary conditions on the surface ($y = 0$) are the no-slip, zero injection conditions: $u(x,0) = 0$ and $\psi(x,0) = 0$ for $t \geq 0$. At the outer edge of the boundary layer ($y \to \infty$) the edge condition on u is $\lim_{y\to\infty} u(x,y;t) \to U_e(x,t)$ and the pressure P satisfies the unsteady Bernoulli relation. The equations can either be solved in direct mode (edge conditions specified) or inverse mode (displacement thickness specified). The additional boundary condition needed for the latter is given by the following relationship between the edge value of ψ and the displacement thickness δ^*,

$$\psi(x, y_e; t) = U_e(x,t)(y_e - \delta^*(x,t)) \ , \tag{5}$$

where y_e is the value of y at the boundary-layer edge and U_e is treated as an unknown. In addition, both upstream and downstream boundary conditions are needed – the latter is required because the introduction of the inviscid normal-momentum equation makes the inviscid form of the governing equations equivalent to the unsteady incompressible Euler equations, which are elliptic-like in space at any time t, as explicitly evidenced by the presence of the ψ_{xx} term in Eq. (4), which represents the streamline curvature. For the simple problem to be considered here, the upstream and downstream profiles for u and ψ are assumed to

correspond to the Blasius (flat-plate) profile. Finally, the initial condition which is needed at time $t = 0$ is assumed to correspond to the Blasius solution along the entire plate surface.

The ITLNS equations are numerically solved using fully implicit discretizations which are first-order accurate for the x- and t-derivatives and second-order accurate for the y-derivatives. All y-derivatives are central differenced and all x- and t-derivatives are backward differenced with respect to the solution point (at (x_i, y_j, t_n)) with the exception of the ψ_{xx} term in the normal-momentum equation, which is central differenced, thus introducing unknown information from the upstream point at x_{i+1}. This information is obtained by initially guessing ψ_{i+1}, using the value from the previous time step, and then performing multiple, global spatial sweeps at each time level until the ψ-field converges. An acceleration scheme has been used to improve the convergence properties of this procedure but will not be discussed here, however, as it is not relevant to the present focus. Initially the authors believed that central differencing of the ψ_{xx} term would properly (and fully) account for the elliptic-like nature of the governing equations at each time step, as demonstrated in applications of similar approaches to steady flows (e.g., see Presz (1985)). However, this was not found to be the case, as will be discussed below.

The issue which is of concern here arises when attempting to solve the above system of equations for a specified time-dependent displacement-thickness distribution (i.e., the inverse method). Consider the simplest possible case, where the displacement thickness is assumed to be that for a steady flat-plate flow for all time $t \geq 0$. Thus, the inverse solution procedure should yield the Blasius solution at all values of x and t, with a small perturbation (depending on the specified value of the Reynolds number) due to normal pressure gradient effects. This has been found to be the case here when the spatial and temporal step sizes Δx and Δt, respectively, are not chosen to be "too small." However, as Δx and Δt are decreased, it has been observed that, during the first time step, the solution departs from its anticipated behavior in a manner reminiscint of that observed when attempting to solve a boundary-value problem using an initial-value technique. This occurs despite the use of central differencing for the ψ_{xx} term. That is, for a fixed, constant spatial stepsize Δx below some minimum value, there appears to be a *minimum* temporal step size Δt, below which the space-marching solution behaves as if it is ill-posed with respect to x.

Examples of the departure solutions are shown in Figs. 1A and 1B, where the skin-friction coefficient, $C_f = 2\tau_w^* \sqrt{Re}/\rho^* U_\infty^{*^2}$, and wall pressure P_w, respectively, are plotted as functions of distance along the plate for a Reynolds number of 1×10^6 based on a reference length $L_{ref} = 1$. This case was calculated starting at $x = 1.0$ with a fixed value of $\Delta x = 0.001$ and three different values of Δt, namely 0.0010, 0.0009 and 0.0001. This value of Δx is below the minimum for which departures have been observed, and the three values of Δt are near the boundary between departure-free solutions and departing solutions. Note that the solution goes from being well-behaved at the largest value of Δt to growing in an oscillatory exponential manner for the middle value to monotonic exponential growth for the smallest value. Similar departure behavior was subsequently observed in the solutions obtained from a different numerical code which uses a similar streamline-curvature based technique to solve the full Navier-Stokes equations, for internal flows, as discussed in the next section.

Before continuing, it should be noted that a consistency check on the finite-difference form of Eq. (4) was carried out. The equations were found to be consistent in the sense that as Δx and Δt are independently reduced to zero, Eq. (4) is identically recovered. Thus, the possibility that truncation errors associated with the discretized equations have changed the mathematical character of the governing differential equations has been eliminated as a possible source for the branching behavior.

Calculations to establish the "departure boundary" for three different Reynolds numbers were performed, namely $Re = 1 \times 10^6$, 1×10^7 and 1×10^8. The results are consistent, and indicate that the value of Δt for which the solution crosses over from "departure-free" to "departing" is a function of Reynolds number, as might be anticipated. The fact that there is a minimum Δx above which solutions remain departure-free for any value of Δt is not surprising – once Δx becomes large enough, the solution probably oversteps the streamwise length scale of the physical mechanism governing the behavior.

The branching behavior of the small step size solutions of the ITLNS equations obtained using the present numerical solution procedure has been examined in detail by the authors in an effort to understand its source. As a result of this investigation, the term responsible for the departure solutions has been found to be the v_t term appearing in the normal-momentum equation. That is, it has been found that, regardless of the values used for Δx and Δt, if the v_t term is *neglected*, then the solution will *never* exhibit the departure behavior described above, so long as the ψ_{xx} term is not backward differenced, but is instead central differenced.

Further, this behavior is found to be independent of the numerical treatment used for the convective terms in the normal-momentum equation.

Recall that in the present study, the v_t term has been written using the stream function definition, i.e., $v_t = -\psi_{xt}$. In the numerical algorithm described above, this term was discretized using a backward difference for the x-derivative, leading to the following form at all y-locations, where the subscript i and superscript n denote the x-index and the t-index, respectively, with (i, n) at the current station in both space and time and Δx assumed to be uniform:

$$\psi_{xt} \approx \frac{1}{\Delta t \Delta x}\left[(\psi_i^n - \psi_{i-1}^n) - (\psi_i^{n-1} - \psi_{i-1}^{n-1})\right] \ . \tag{6}$$

The apparent ill-posedness exhibited by the numerical solutions, and the fact that the v_t term has been found to be responsible, suggests an alternative discretization for the ψ_{xt} term wherein a *forward* difference in x with respect to the solution station is used. That is, ψ_{xt} is discretized in the form

$$\psi_{xt} \approx \frac{1}{\Delta t \Delta x}\left[(\psi_{i+1}^n - \psi_i^n) - (\psi_{i+1}^{n-1} - \psi_i^{n-1})\right] \ . \tag{7}$$

With this modification, the ill-posed behavior which is observed when a backward difference is used no longer arises, regardless of the values of Δx and Δt that are specified. A case for which violent branching occurs when using a backward difference for the x-derivative in ψ_{xt}, which was presented in Fig. 1, has been recalculated using a forward difference with the same spatial and temporal stepsizes, i.e., $\Delta x = 0.001$ and $\Delta t = 0.0001$. The resultant solution is departure free and virtually identical to the backward-difference solution for $\Delta t = 0.001$, which did not branch because the value of Δx was too large.

The precise reason that forward-differencing of the x-derivative in the ψ_{xt} term is needed to prevent the ill-posed behavior of the small step-size solutions of these equations is unknown at the present time. One possiblity is that the responsible mechanism is somehow related to physical boundary-layer instability mechanisms. Another possibility is that the mechanism is purely inviscid in nature, as is the case leading to the requirement for central differencing of the ψ_{xx} term. Both of these possiblities are currently under investigation, and it is hoped that this issue will be resolved in the near future.

Internal Flow Analysis – Pulsatile Flow Through a Channel

Here the governing equations are taken to be the unsteady Navier-Stokes equations. This set of equations is non-dimensionalized by the method of Smith (1976). The final equations are: conservation of mass,

$$u_x + v_y = 0 \ ; \tag{8}$$

conservation of x-momentum,

$$u_t + Re(uu_x + vu_y) = -P_x + \underline{u_{xx}} + u_{yy} \ ; \tag{9}$$

and conservation of y-momentum,

$$\underline{v_t} + Re[u(v_x - v_T) + \underline{vv_y}] = -P_y + \underline{v_{xx}} + \underline{v_{yy}} \ . \tag{10}$$

The v_T term is a pseudo-time derivative introduced to accelerate convergence of the global-iteration scheme at each time-level t. The Reynolds number, Re, is defined here by $Re = L^{*3} g^* / \rho^* \nu^{*2}$, where L^* is the dimensional channel width, ρ^* is the density, ν^* is the kinematic viscosity and $-g^*$ is the local applied pressure gradient driving the basic flow. This set of equations is solved in a two-dimensional channel where the upstream flow is a pulsatile Poiseuille flow driven by the pressure gradient

$$\frac{\partial P}{\partial x}(-\infty, y) = -1 + \gamma_0 \cos \beta t \ . \tag{11}$$

The corresponding velocity profile is

$$u(-\infty, y) = u_0^s + u_0^u \ , \tag{12}$$

where

$$u_0^s = \frac{1}{2} y(1 - y) \qquad , \quad u_0^u = c_1 e^{\sqrt{\beta} e^{\frac{i\pi}{4}} y} + c_2 e^{\sqrt{\beta} e^{\frac{3i\pi}{4}} y} - \frac{\gamma_0}{2i\beta} \ , \tag{13}$$

with

$$c_1 = \frac{e^{\sqrt{\beta}e^{\frac{5\pi i}{4}}}}{2i\beta\left[1+e^{\sqrt{\beta}e^{\frac{5\pi i}{4}}}\right]} \quad , \quad c_2 = \frac{\gamma_0}{2i\beta\left[1+e^{\sqrt{\beta}e^{\frac{5\pi i}{4}}}\right]} \tag{14}$$

and $v(-\infty, y) = 0$. No-slip boundary conditions are applied along the upper and lower walls and the downstream boundary conditions are $u_x = 0$ and $v_x = 0$.

For the case where the streamwise length scale is the same order as the channel width, the minimal system of equations needed to reproduce the unsteady asymptotic structure of Smith (1976) is the parabolized Navier-Stokes (PNS) equations (Eqs. (8)-(10) with all underlined terms neglected). Bearing this in mind, a Navier-Stokes algorithm is formulated by first developing a PNS algorithm and then iterating on the additional (underlined) terms. It is well-known that, when solving the *steady* PNS equations, departure solutions can be suppressed either by neglecting the streamwise pressure-gradient term P_x, or the streamline-curvature term (the uv_x term, see Rothmayer (1989, 1990)). In this study, the streamline-curvature term uv_x is used to suppress departure solutions in the steady single-pass version of the algorithm, and also to provide a mechanism for upstream propagation of information in the steady and unsteady global-iteration algorithms.

The streamline-curvature term uv_x is treated as a known source term and is forward-differenced in space relative to the current solution point. The pseudo-unsteady term uv_T (introduced to accelerate convergence as in Davis (1984) and Barnett and Davis (1986)) is included implicitly using a standard backward difference in time (see Rothmayer (1989, 1990)). Note that two unsteady effects are present – the real unsteady terms u_t and v_t and the pseudo-unsteady term v_T. The latter is driven to zero during multiple sweeps through the solution domain at each real time level t.

The algorithm described above, without the addition of the Navier-Stokes terms (i.e., underlined terms in Eqs. (8)-(10)) is similar to that described in the section on external flows, where the ITLNS equations are solved. As with that algorithm, a number of implicit/explicit PNS-like algorithms were tested. The full Navier-Stokes version of the internal-flow solution technique treats the underlined terms as source terms calculated from the solution at the previous iteration, although algorithms with implicit treatment of v_t were also tested. The reader is referred to Rothmayer (1990) for further details.

The above-described Navier-Stokes solution algorithm has been used to solve for the flow through a flat channel with the pulsatile pressure gradient given by Eq. (11) and the upstream boundary conditions given by Eqs. (12–14). Fig. 2A shows a comparison between the wall shear stress computed using the present analysis at a downstream location along with that given by the analytical Poiseuille solution – the agreement is excellent. The departure solutions, to be discussed next, were triggered by introducing a very small indentation in the channel wall (typical height $h = 1 \times 10^{-6}$).

As with the previously described external-flow analysis, it has been found that the present solution algorithm experiences departure-solution behavior when a minimum spatial/temporal step-size restriction is violated, with solutions like that shown in Fig. 1. Figure 2B shows how the minimum allowable time step, Δt_s, changes with varying streamwise step size, Δx, for a Reynolds number of 10 million. For a streamwise step size above a critical value ($\Delta x \approx 0.207$) the numerical scheme is free of departure solutions for all values of Δt examined. As found with the external-flow analysis, neglecting the v_t term leads to departure-free solutions for all values of Δx and Δt.

A similar departure-solution behavior was also observed when solving the PNS equations numerically. As with the Navier-Stokes algorithm, the unsteady PNS method displayed the spatial/temporal step-size constraints. These departure solutions could again be eliminated by neglecting the v_t term. These observations hold even if the normal-momentum equation is reduced to the very simple form $v_t = -P_y$.

In the external-flow analysis, branching of the numerical solution was suppressed by spatially forward-differencing the v_t term, after re-expressing in terms of the stream function. A similar approach was attempted in the internal-flow analysis. The $-\psi_{xt}$ term was forward and backward differenced in space, and treated both implicitly and explicitly in both cases, in an attempt to eliminate the departure solutions. Of the four methods, the backward-differenced explicit method had the least severe time-step restriction for a given value of Δx. However, for sufficiently small time steps, all four algorithms exhibited the departure-solution behavior previously discussed. This is in contrast with the external-flow analysis, where branching could be completely eliminated by spatial forward-differencing of the $-\psi_{xt}$ term. It is not clear at this time

why this difference between the internal- and external-flow analyses exists. Fortunately, the pseudo time step ΔT can be optimized so that the time scales for the observed departure solutions fall below the scales of the Navier-Stokes regime (which constitute a likely absolute lower bound on the temporal time step needed for practical calculations). However, if a judicious choice of ΔT is not made, then departure solutions may be encountered even at the large values of Δt associated with the interactive boundary-layer regime of Smith (1976) (see Fig. 2C).

Another interesting, and currently unexplained, phenomena observed in both the internal- and external-flow analyses is that departure solutions can be eliminated by neglecting the v_t term in certain local transverse regions, while retaining this term outside of those regions. The five points labeled A1, A2 and B1 through B3 on Fig. 2B are points at which the solution has been stabilized by neglecting v_t in the various regions indicated. Fig. 2D shows the location of these regions for each point. It can be seen from this group of figures that the size and location of these regions are sensitively dependent on both the spatial and temporal stepsizes. For all values of Δx there appears to exist a Δt below which v_t must be neglected across the entire channel to ensure departure-free solutions.

Concluding Remarks

The objective of this paper has been, first, to describe departure solution behavior observed when using streamline-curvature based solution procedures which are being developed to study high Reynolds number vortex-eruption phenomena, second, to indicate the responsible term in the governing equations and, finally, to show how the departure solutions can be eliminated. We have shown that the time-derivative of the normal velocity, $v_t = -\psi_{xt}$, appearing in the normal-momentum equations, is responsible for the branching behavior, which only occurs for small spatial and temporal step sizes. The ill-posed behavior has been eliminated in the external-flow analysis by forward differencing the spatial-derivative appearing in the $-\psi_{xt}$ term. It should be noted that the step sizes for which the observed ill-posed behavior arises turn out to be within the range needed to capture many important unsteady viscous-inviscid interaction phenomena, such as dynamic stall onset. Therefore, this mechanism should not be ignored if accurate solutions are to be obtained. The implication is that special differencing procedures may be needed to properly account for the mechanisms responsible for the elliptic-like character of the governing equations at each time level of a time-marching algorithm, possibly even for non-streamline-curvature techniques. A more complete description of the responsible mechanism is currently being pursued by the authors, and will be reported when it is available.

Acknowledgements

The authors wish to acknowledge the helpful discussions of Dr. Frank Smith of University College, London and Mr. Robert LaBarre of UTRC. We also wish to gratefully acknowledge the funding of this research by the United Technologies Corporation and by the National Science Foundation Presidential Young Investigator Award of A. P. Rothmayer. Finally, the authors would like to acknowledge the computational resources provided by the Iowa State University Computation Center.

References

Barnett, M. and Davis, R. T., 1986, "Calculation of Supersonic Flow with Strong Viscous-Inviscid Interaction," *AIAA J.*, **24**, pp. 1949–1955.

Davis, R. T., 1984, "A Procedure for Solving the Compressible Interacting Boundary-Layer Equations for Subsonic and Supersonic Flows," AIAA Paper 84–1614.

Elliott, J. W., Cowley, S. J. and Smith, F. T., 1983, "Breakdown of Boundary Layers: (i) On Moving Surfaces, (ii) In Semi-Similar Unsteady Flow, (iii) In Fully Unsteady Flow," *Geophys. and Astrophys. Fluid*

Dyn., **25**, pp. 77–138.

Peridier, V. J., Smith, F. T. and Walker, J. D. A., 1988, " Methods for the Calculation of Unsteady Separation," AIAA paper 88–0604.

Power, G. D., 1990, "A Novel Approach for Analyzing Supersonic High Reynolds Number Flows with Separation," AIAA Paper 90–0764.

Presz, W. M., 1985, "A Numerical Method for Duct Flow with Boundary-Layer Separation," AIAA Paper 85–1410.

Rothmayer, A. P., 1989, "The Computation of Separated Flows in Symmetric Channels," Proceedings of the Fourth Symposium on Numerical and Physical Aspects of Aerodynamic Flows, Long Beach, CA.

Rothmayer, A. P., 1990, "Solution of the High Reynolds Number Navier-Stokes Equations by Global Streamline Curvature Iteration," to appear in *Eur. J. Mech.*

Smith, F. T., 1976, "Flow Through Constricted or Dilated Pipes and Channels: Parts 1 and 2," *Q. Journal Mech. Appl. Math.*, **29(3)**, pp. 343–364.

Smith, F. T., 1979, "On the Non-Parallel Flow Stability of the Blasius Boundary Layer," *Proc. Roy. Soc.* **A366**, pp. 91–109.

Smith, F. T., 1988, "Finite-Time Breakup Can Occur in any Unsteady Interacting Boundary Layer," *Mathematika*, **35** pp. 256–273.

Smith, F. T., Papageorgiou, D. and Elliott, J. W., 1984, "An Alternative Approach to Linear and Nonlinear Stability Calculations at Finite Reynolds Numbers," *J. Fluid Mech.*, **146**, pp. 313–330.

van Dommelen, L. L. and Shen, S. F. 1980, "The Spontaneous Generation of the Singularity in a Separating Laminar Boundary Layer," *J. Comp. Phys.*, **38**, 125.

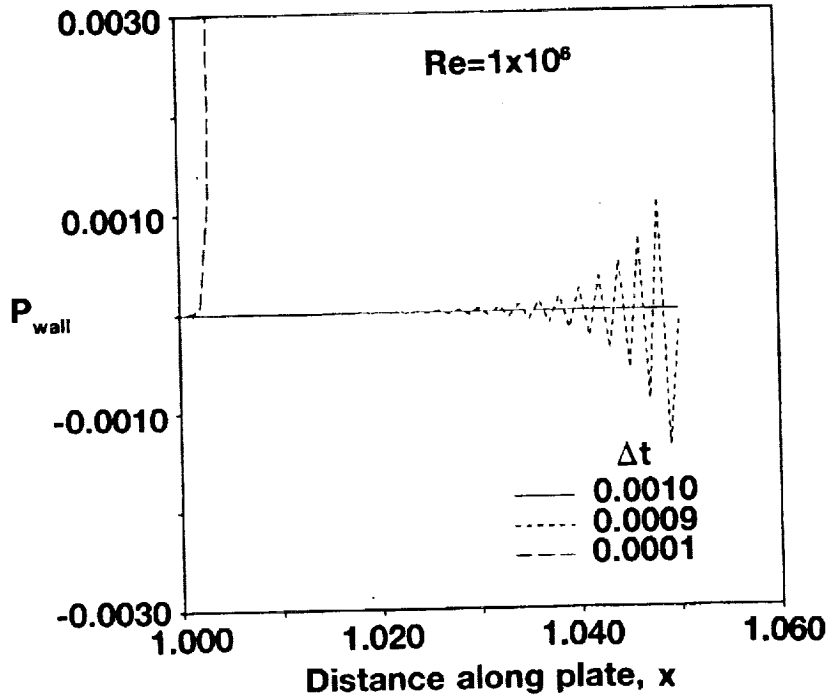

Fig. 1A. Wall pressure along plate for three values of Δt, Δx=0.001.

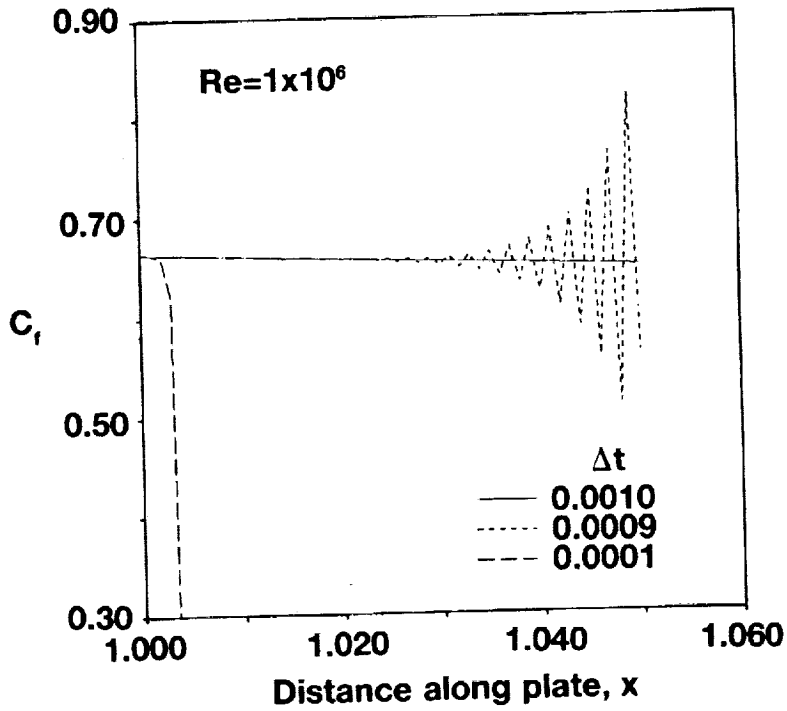

Fig. 1B. Skin-friction coefficient along plate for three values of Δt, Δx=0.001.

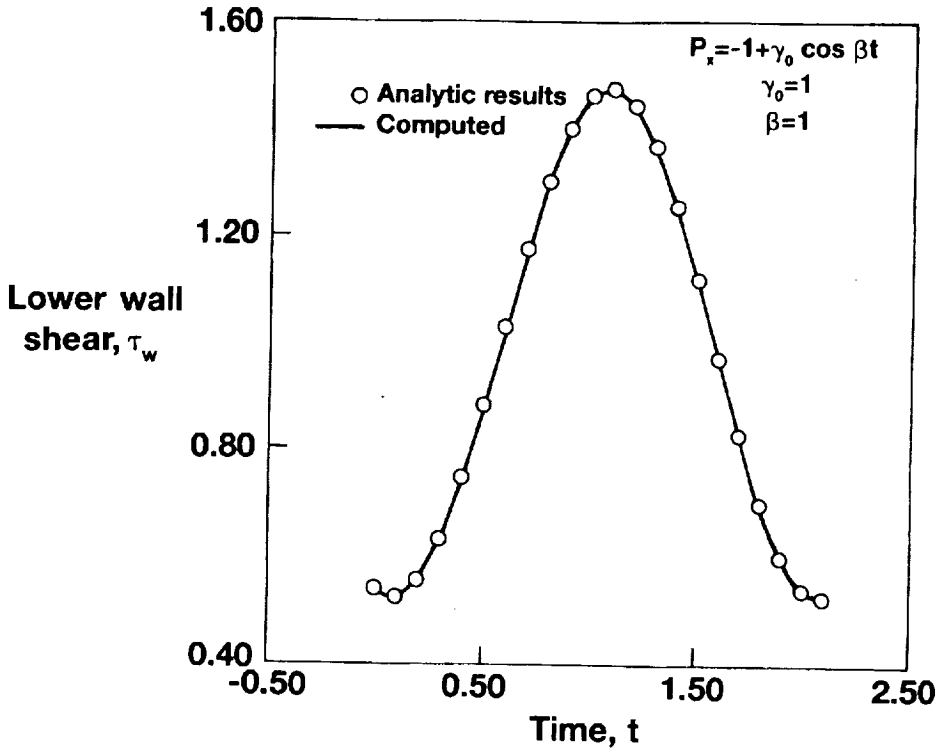

Fig. 2A. Comparison of analytical and calculated wall shear with the solution driven by a pulsatile pressure gradient.

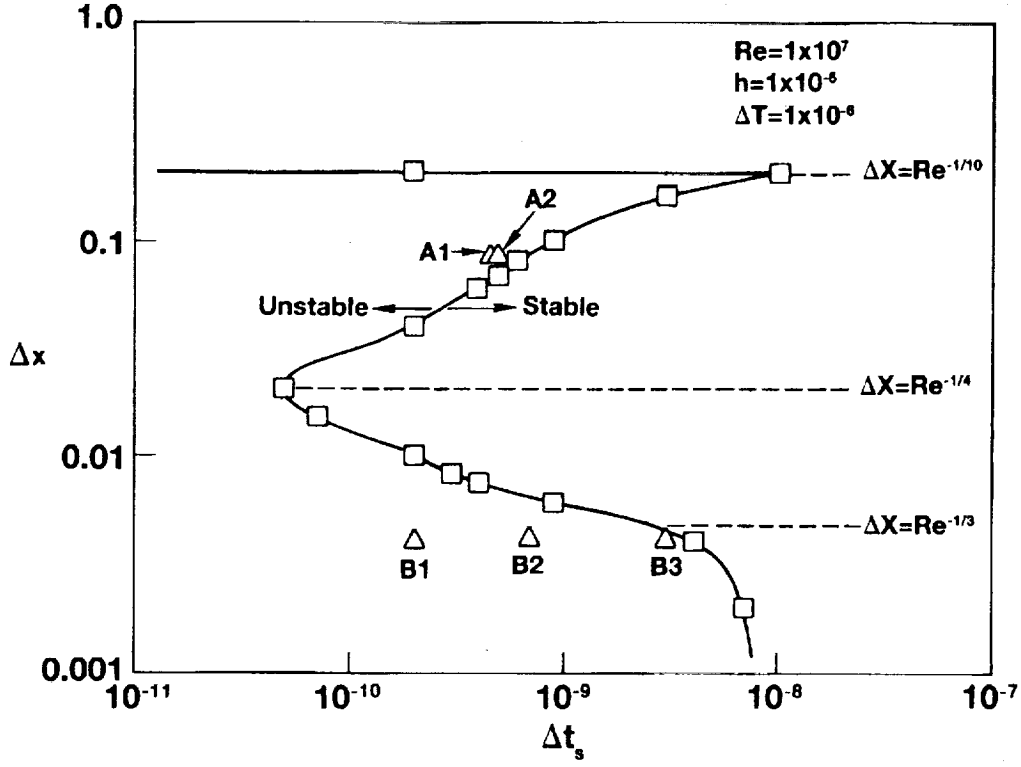

Fig. 2B. Stability boundary for the internal flow algorithm.

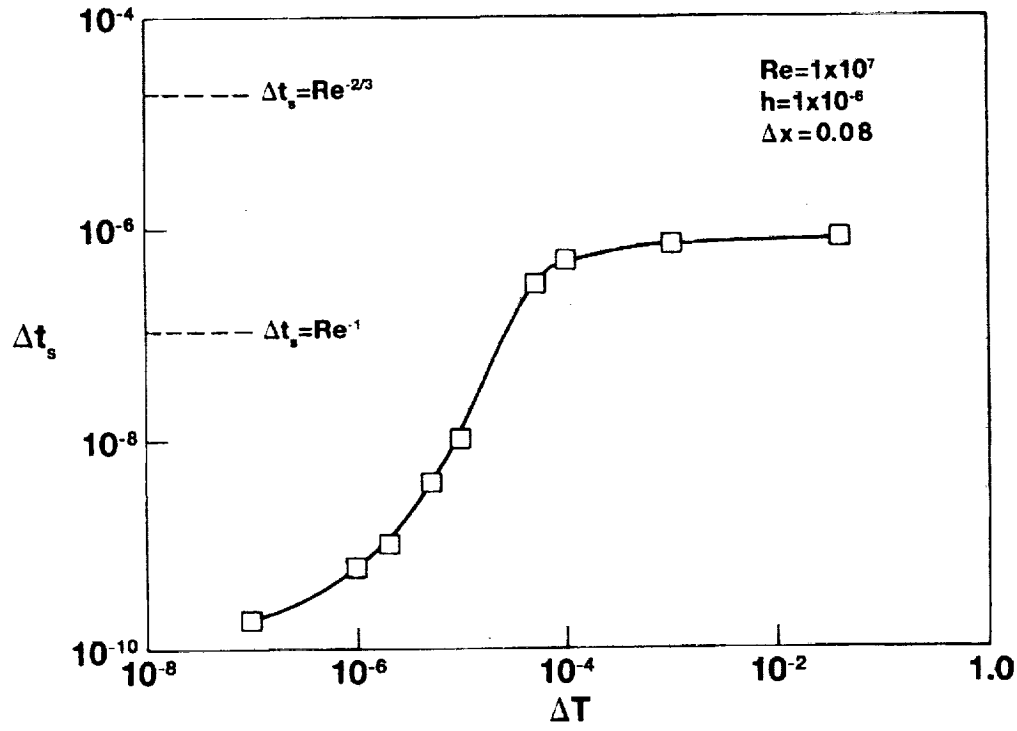

Fig. 2C. Variation of minimal time step constraint with changing pseudo time step.

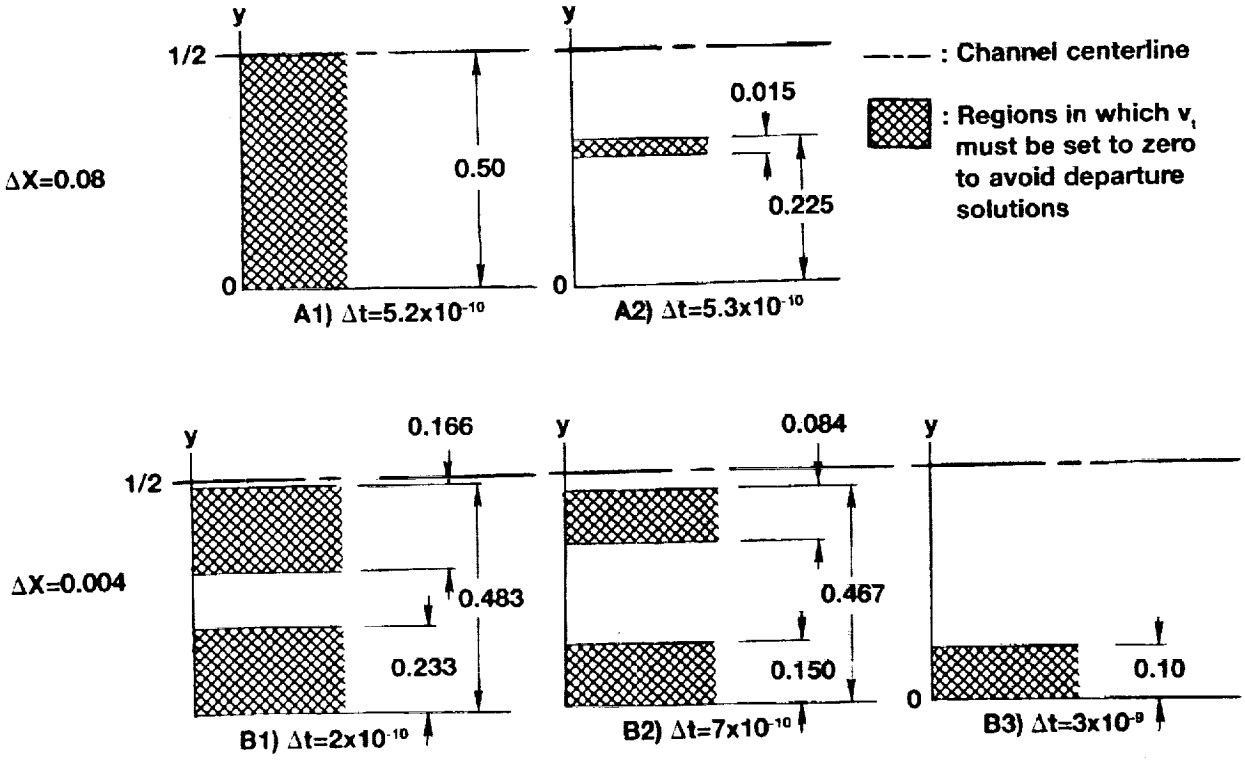

Fig. 2D. Illustration of regions where neglecting V_t suppresses branching.